



**UNIVERSITI PUTRA MALAYSIA**

**EX VIVO CORRELATION OF ULTRASONOGRAPHIC APPEARANCE OF  
GASTRIC SUBMUCOSAL FAT WITH HISTOLOGY IN CATS**

**TEOH YONG BIN**

**Ip  
FPV 2017 66**

**EX VIVO CORRELATION OF ULTRASONOGRAPHIC APPEARANCE OF GASTRIC  
SUBMUCOSAL FAT WITH HISTOLOGY IN CATS**



**TEOH YONG BIN**

**FACULTY OF VETERINARY MEDICINE**

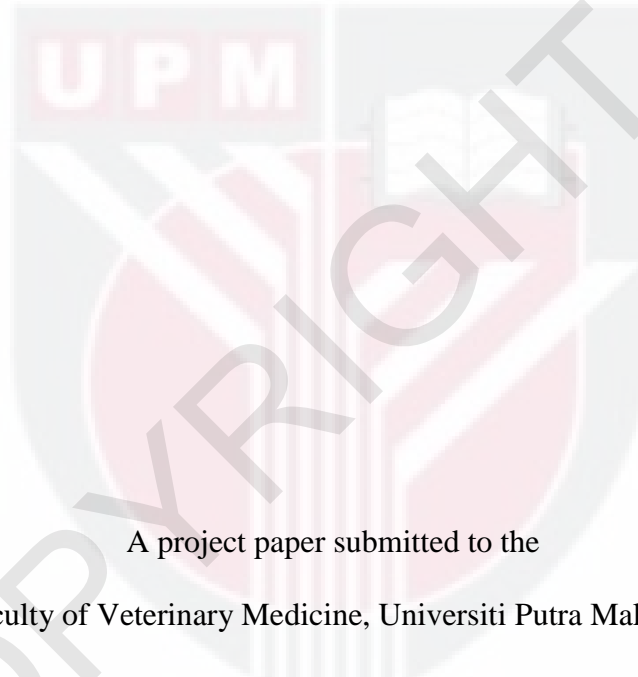
**UNIVERSITI PUTRA MALAYSIA**

**SERDANG, SELANGOR**

**MARCH 2017**

**EX VIVO CORRELATION OF ULTRASONOGRAPHIC APPEARANCE OF  
GASTRIC SUBMUCOSAL FAT WITH HISTOLOGY IN CATS**

**TEOH YONG BIN**



A project paper submitted to the  
Faculty of Veterinary Medicine, Universiti Putra Malaysia

In partial fulfillment of requirement for the  
**DEGREE OF DOCTOR OF VETERINARY MEDICINE**

Universiti Putra Malaysia,  
Serdang, Selangor Darul Ehsan.

MARCH 2017

## CERTIFICATION

It is hereby certified that we have read this project paper entitled “Ex Vivo Correlation of the ultrasonographic appearance of gastric submucosal fat with histology in cats”, by Teoh Yong Bin and in our opinion it is satisfactory in terms of scope, quality, and presentation as partial fulfillment of the requirement for the course VPD 4999 - Project

---

DR. LIM SUE YEE

DVM (UPM), Ph.D. (Hokkaido)

Senior lecturer

Faculty of Veterinary Medicine

Universiti Putra Malaysia

(Supervisor)

---

DR. MAZLINA MAZLAN

DVM (UPM), M.Sc. (UPM), Ph.D. (UPM)

Senior lecturer

Faculty of Veterinary Medicine

Universiti Putra Malaysia

(Co-Supervisor)

## DEDICATIONS

*To The Triple Gems,*

*The Buddha, the holy one, the fully enlightened one,*

*The Dhamma, His teachings which have guided my path,*

*The Sangha, the Order of monks which have pointed me to the Eight-Fold Path.*

To my family,

Teoh Jin Eng,

Tan Phaik Hong,

Teoh Mei Xian,

Teoh Yong Jun,

Teoh Mei Xing,

Ng Jia Chen,

Jessica Ng You Rou

And to all sentient beings perfecting their minds to be free from Samsara.

## ACKNOWLEDGEMENTS

A million of thanks to Dr Lim Sue Yee, for her kindness and patience in guiding me as a student and a novice in ultrasonography; for her attentiveness during the times when I was lost and needed a point towards the right direction; for her brilliance and knowledge in all aspects of veterinary medicine and life in opening up the views and horizons I could never have seen; and for her trust given to me as a student and fellow colleague in completing this project.

A tremendous amount of appreciation to Dr Mazlina Mazlan, for her undying support throughout the strenuous period of the project especially in the skills of histopathology; for her open mind to guide me off all my previous ignorance towards the art of histopathology; for her optimism towards all the plunders I have met throughout the histopathological processing; and for her trust given to me as a student and fellow colleague in completing this project.

A never-ending thoughts of gratitude to Dr Tan Li Ping, Michelle who have given an immense amount of her effort and time throughout her Masters program to work with me throughout the project. Going through the good times, bad times, stressful times and joyful times with a sister I never had was a definitely a gift I could never had asked for more during the project period.

Many thanks for the Staffs of DBKL Pest Unit, Staffs of PAWS, Staffs of Histopathology Lab and Dr Muhamad Alif Zakaria, Staffs of Necropsy Lab and Professor Dr Noordin Mohamed Mustapha, Staffs of Radiology Unit and Dr Lau Seng Fong and the Staffs of Clinical Lab and Associate Prof. Dr Faez Firdaus Jesse Abdullah for the positive support given to me to complete the project.

A heartfelt thank you to Professor Dr Mohamed Ariff Omar and Associate Prof. Dr Goh Yong Meng, for the time and patience in deciphering the statistical portion of the project with me.

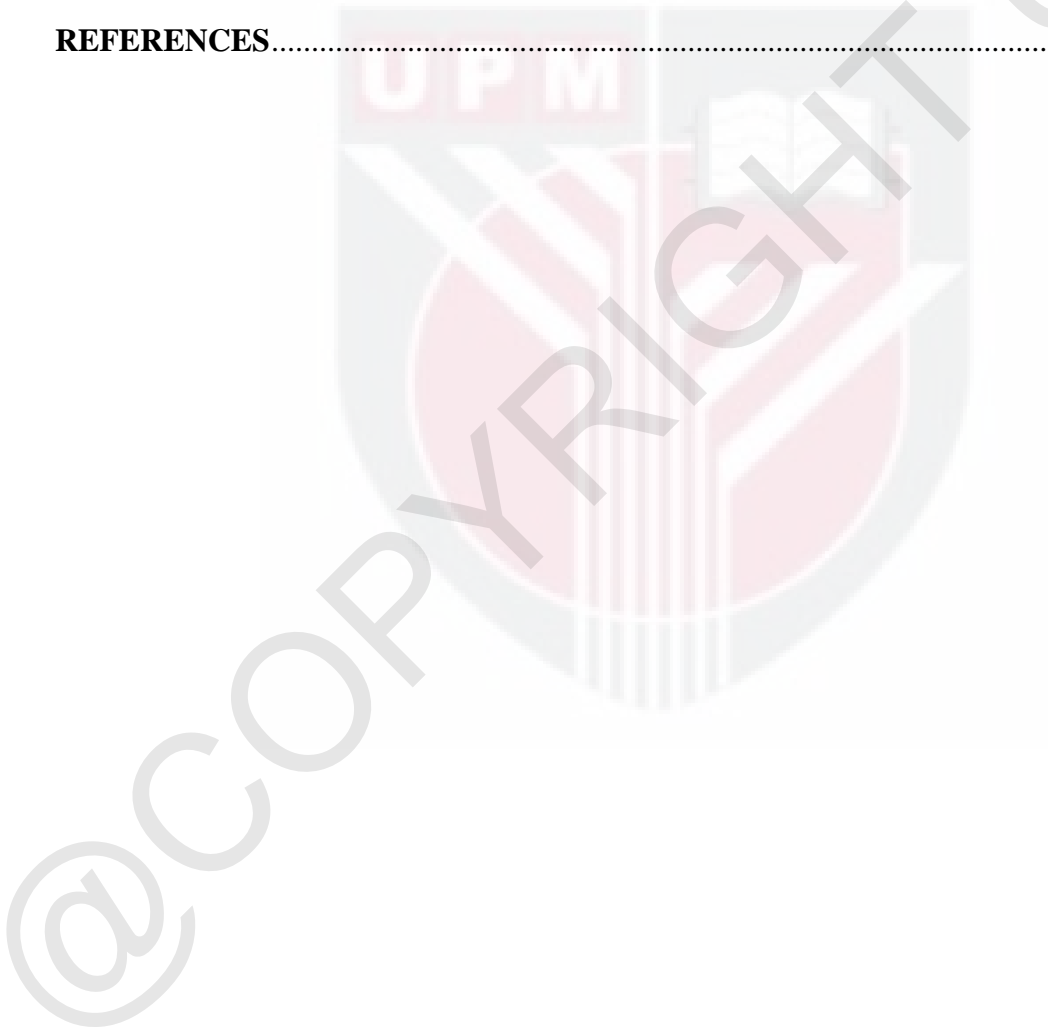
A shout out of thank you to DVM Class of 2016 and 2017, Vet-souls and Kaki Jalan who have given the attention and advices throughout the midst of the project to keep me mentally charged and going.

Last but not least, I would also like to thank my family for the understanding and support given in various ways for me to complete this project, as well as my good friends Lam Jer Renn, Heng Jia Wei and Wong May Yuan who have inspired me to be who I am today to complete the project.

## CONTENTS

	<b>Page</b>
<b>TITLE</b> .....	i
<b>CERTIFICATION</b> .....	ii
<b>DEDICATIONS</b> .....	iii
<b>ACKNOWLEDGEMENTS</b> .....	iv
<b>CONTENTS</b> .....	vi
<b>LIST OF TABLES</b> .....	viii
<b>LIST OF FIGURES</b> .....	viii
<b>ABSTRACT</b> .....	ix
<b>1.0 INTRODUCTION</b> .....	1
<b>2.0 LITERATURE REVIEW</b> .....	3
2.1 Gross anatomy of the stomach.....	3
2.2 Histology of gastric layers.....	4
2.3 Uses of Ultrasonography in Gastrointestinal Disorders.....	4
2.4 Ultrasonography of Gastric Layers.....	5
2.5 Pathologies associated to gastrointestinal layer changes ultrasonographically....	6
2.6 Emerging Changes in Gastric Submucosal Thickness.....	7
2.7 Gastric Submucosal Fat Detection by Radiograph and CT Scan.....	7
2.8 Gastric attachment to the adjacent organs.....	8
<b>3.0 MATERIALS AND METHODS</b> .....	9
3.1 Animals.....	9
3.2 Lipid Profiling.....	9
3.3 In-vivo Ultrasound.....	10
3.4 Organ Procurement.....	11
3.5 Ex-vivo Ultrasound.....	11
3.6 Histology.....	13

3.7	Quantitative Analysis.....	13
3.9	Statistical Analysis.....	15
<b>4.0</b>	<b>RESULTS</b> .....	<b>16</b>
4.1	Animals .....	16
4.2	Stomach samples .....	16
4.3	Histology Samples.....	16
4.4	Ultrasonographic and Histological Statistical Analysis .....	16
<b>5.0</b>	<b>DISCUSSION</b> .....	<b>21</b>
<b>6.0</b>	<b>CONCLUSION</b> .....	<b>24</b>
	<b>REFERENCES</b> .....	<b>25</b>



**LIST OF TABLES**

	<b>Page</b>
Table 1: Thickness of the Fundus, Body and Pylorus Wall Layers Measured in Ultrasonography and Histologically .....	17
Table 2: Distribution of Fat Score in Submucosa Layer in different regions of the stomach .....	17
Table 3: Correlation of Gastric Submucosa Layer Thickness between Ultrasonography and Histology.....	17
Table 4: Association between Gastric Submucosal Layer Thicknesses on Ultrasonography (GSM <sub>US</sub> ) at the Presence of Rugae Fold.....	18
Table 5: Association between Gastric Submucosal Layer Thickness in Ultrasonography (GSM <sub>US</sub> ) to Gastric Submucosal Fat Score in Histology.....	18
Table 6: Association between Serum Lipid Parameters to Gastric Submucosal Fat Score Measurements in Histology.....	18

**LIST OF FIGURES**

	<b>Page</b>
Figure 1: Estimation Table of Dentition of Cats .....	9
Figure 2: Three different regions of ultrasonographic imaging .....	12
Figure 3: Fat score table derived from Heng <i>et al.</i> , 2008.....	15
Figure 4: Scatterplot of GSM <sub>US</sub> against GSM <sub>HS</sub> in the body.....	19
Figure 5: Scatterplot of GSM <sub>US</sub> against GSM <sub>HS</sub> in the fundus .....	19
Figure 6: Scatterplots of GSM <sub>US</sub> against GSM <sub>HS</sub> in the pylorus .....	19
Figure 7: Ultrasonographic image of gastric with presence of rugae fold.....	20
Figure 8: Ultrasonographic image of gastric with absence of rugae fold .....	20
Figure 9: Histological image of gastric submucosa with fat score of 0 .....	20
Figure 10: Histological images of gastric submucosa with fat score of 4 .....	20

**ABSTRACT**

An abstract of the project paper presented to the Faculty of Veterinary Medicine in partial fulfilment of the course VPD 4999 – Project.

**EX VIVO CORRELATION OF ULTRASONOGRAPHIC APPEARANCE OF  
GASTRIC SUBMUCOSAL FAT WITH HISTOLOGY IN CATS****By****Teoh Yong Bin****2017****Supervisor: Dr. Lim Sue Yee****Co-Supervisor: Dr. Mazlina Mazlan**

**Background:** Ultrasonographic assessment of the stomach and its layers are performed routinely in companion animals. Varying submucosal thicknesses are seen in cats ultrasonographically, however their attribution to fat deposition, anatomical variation or disease processes remain unknown.

**Hypothesis/Objective:** To correlate appearance of gastric submucosa on ultrasound with its histology in cats.

**Animals:** 25 cats from animal shelters and pounds.

**Methods:** Following humane euthanasia for various reasons, the stomach was resected and ex-vivo ultrasonography was performed at the fundus, body and pylorus. Ultrasound measurements include thickness of gastric wall ( $GW_{US}$ ) and submucosa ( $GSM_{US}$ ). Gastric rugae fold (RF) presence was also recorded. Thereafter, histology of the stomach section measured at ultrasound was performed. Histological measurements include thickness of gastric wall ( $GW_H$ ) and submucosa ( $GSM_H$ ) and submucosa fat score ( $GSM_{FAT}$ ).

**Results:** Fat was present in the gastric submucosa in 96% of cats. However, no association was found between  $GSM_{US}$  and  $GSM_{FAT}$  in all regions.  $GSM_{US}$  was correlated to  $GSM_H$  ( $r=0.459$ ;  $P=0.021$ ) in the body. RF was associated to  $GSM_{US}$  in fundus and body.

**Conclusion:** Gastric submucosal thickness is not associated to fat deposition on histology. Nevertheless, ultrasonographic thickness in gastric submucosa corresponds to histology and was also associated to presence of rugae fold.

**Keywords:** Cat, Histology, Stomach, Submucosa, Ultrasound



**ABSTRAK**

Abstrak daripada kertas projek yang dikemukakan kepada Fakulti Perubatan Veterinar untuk memenuhi sebahagian daripada keperluan kursus VPD 4999 – Projek.

**KORELASI EX VIVO ANTARA KEMUNCULAN LEMAK SUBMUKOSA GASTRIK  
DI ULTRASOUND DENGAN HISTOLOGI DALAM KUCING**

Oleh

**Teoh Yong Bin**

**Penyelia: Dr. Lim Sue Yee**

**Penyelia bersama: Dr. Mazlina Mazlan**

**Latar belakang:** Taksiran ultrasound perut serta lapisannya sudah digunakan secara rutin dalam haiwan kesayangan. Ketebalan submukosa yang berbeza telah dijumpai dalam ultrasound, namun atribusi kepada perbezaan ini dari segi pengendapan lemak, variasi anatomi ataupun proses penyakit masih tidak diketahui.

**Hipotesis/Objektif:** Untuk mengkorelasikan penemuan submukosa gastrik melalui ultrasound dengan histologi dalam kucing.

**Haiwan:** 25 ekor kucing dari pusat perlindungan dan pusat pengurangan haiwan.

**Kaedah:** Selepas euthanasia secara berperikemanusiaan dibuat atas pelbagai sebab, perut telah diresek dan penskanan ultrasound secara ex vivo telah dibuat pada bahagian fundus, badan dan pilorus. Ukuran ultrasound yang diperolehi termasuk ketebalan dinding gastrik ( $GW_{US}$ ) dan submukosa ( $GSM_{US}$ ). Kehadiran lipatan ruga gaster (RF) turut direkodkan. Seterusnya, histologi pada keratan perut yang telah diukur melalui ultrasound dibuat. Ukuran histologi yang

diambil termasuklah ketebalan dinding gastrik ( $GW_H$ ) dan submukosa ( $GSM_H$ ) serta skor lemak submukosa ( $GSM_{FAT}$ ).

**Keputusan:** Kajian mendapati lemak hadir dalam submukosa gastrik dalam 96% daripada sampel kucing yang dikaji. Namun, tiada perkaitan dijumpai antara  $GSM_{US}$  dengan  $GSM_{FAT}$  dalam kesemua kawasan perut. Terdapat korelasi antara  $GSM_{US}$  dan  $GSM_H$  ( $r=0.459$ ;  $P=0.021$ ) hanya pada sampel daripada bahagian badan perut. RF juga mempunyai korelasi dengan  $GSM_{US}$  pada bahagian fundus dan badan perut.

**Kesimpulan:** Penemuan menunjukkan tiada kaitan antara ketebalan submukosa gastrik dengan pengendapan lemak dalam histologi. Walaubagaimanapun, ketebalan submukosa gastrik melalui penskanan ultrasound berpadanan dengan histologi dan turut dipengaruhi oleh kehadiran lipatan ruga.

**Kata kunci:** Kucing, Histologi, Perut, Submukosa, Ultrasound

## 1.0 INTRODUCTION

Gastric wall assessment is routinely performed using ultrasonography. Ultrasonographically established layers include hyperechoic lumen/mucosal surface, hypoechoic mucosa, hyperechoic submucosa, hypoechoic muscularis propria and lastly hyperechoic serosa (Pennick *et al.*, 1989). Some ultrasonographic changes in gastrointestinal tract layer thickness and echogenicity have been reported as related to pathology, i.e. increased muscularis layer thickness have been reported in cats with inflammatory bowel diseases (Larson *et al.*, 2009). Imaging studies in people have reported presence of gastric fat halo sign observed in computed tomography (CT) and have associated this finding with inflammatory bowel diseases such as Crohn Disease and Ulcerative Colitis (Ahuali, 2008). However, another study described this finding as gastric wall fatty infiltration that may be a normal finding (Gervaise, 2016).

In cats, these gastric radiolucent bands on radiography and gastric hypoattenuating layer on CT scans seen in cats with no overt gastrointestinal signs of disease are associated to gastric wall fatty infiltration as confirmed with histology (Heng *et al.*, 2005 and 2008). This finding corresponds to the gastric fat halo sign as seen in human studies.

On ultrasound, the gastric submucosal layer is hyperechoic (Anderson, 2011). Variations in submucosal thickness are seen ultrasonographically in cats. It is unknown if this variation is anatomical or attributed to disease process. Therefore, there remains a need to correlate ultrasonographic appearance of the gastric submucosal layer with disease process or with anatomical variation using histology as gold standard.

The objectives of this studies are:-

- 1) To correlate the appearance of gastric submucosal fat with ultrasonography and histology in terms of thickness

- 2) To determine the association between the gastric submucosal thickness in ultrasonography to gastric submucosa fat deposition in terms of fat score
- 3) To determine the association between the presence of rugae fold in ultrasonography to gastric submucosal thickness in ultrasonography
- 4) To determine the association between the serum lipid parameters to gastric submucosal fat deposition in terms of fat score.



## 2.0 LITERATURE REVIEW

### 2.1 Gross anatomy of stomach

Cats are carnivorous mammals with a simple stomach that allows the consumption of a concentrated diet, easiest to digest among all mammals (Dyce *et al.*, 2002). Grossly the cardia, fundus and pylorus compose the stomach which connects proximally from the esophagus at the cardia to receive ingesta (Dyce *et al.*, 2002). Cardia is named after its proximity to the heart, for which it is located under cover of the ribs on the left median plane (Akers & Denbow, 2008). Fundus forms the blind dome proximal to the cardia while the body (corpus) extends towards the ventral angle from the cardia to function as a mixing region for the stomach. The smaller part of the stomach, namely the pylorus, is made of the proximal pyloric antrum and distal pyloric body, for which it is not affected by the presence of a meal. Subsequently, the tubular structure forms a narrower lumen and thicker wall which projects towards the duodenum (Dyce *et al.*, 2002).

In cats, the stomach starts with an outermost layer covering the whole organ known as the external peritoneum or serosa, which adheres to the underlying muscles. The subsequent layer is composed by smooth muscles, named as the muscularis layer. The muscularis layer is a composite of an outer longitudinal, middle circular and inner oblique muscle layer. Submucosal walls are depicted as layers of connective tissue mainly made of elastic collagen fibres, arterial and venous plexuses (Dyce *et al.*, 2002). A layer named muscularis mucosae plexiform connects the submucosa to the mucosal proper. The muscularis mucosae plexiform is aided by the elastic fibers of submucosa to propel mucosa of empty stomach organ into folds, forming the rugae surfaces. In the relaxed state, the inner surface of the stomach upon cut section will reveal prominent folds named as the rugae on the stomach mucosa. When the stomach expands after meal consumption, the rugae will flatten out and no longer be prominent.

## 2.2 Histology of gastric layers

Layers of the stomach, are correlated significantly between ultrasonography and histology. Histologically, all layers of the stomach are formed to allow the specialized function of the organ to perform enzymatic and hydrolytic breakdown of ingesta. From the lumen, the layers of stomach are made up of the mucosa, submucosa, muscularis and the serosa. The mucosal layer receives the secretory products from gastric pits for the breakdown mechanisms of the ingesta (Dyce *et al.*, 2002). The next layer after the gastric mucosa is composed by the submucosa which contains collagen fibers, white adipose tissue and blood vessels (Frappier, 2006). Within the submucosa, presence of vascular plexus give rise to the mucosal capillary bed. Meissner's plexus found in the submucosa act as the branch of autonomic nervous system for the control of muscularis mucosae layer (King, 2009) as well as glandular secretion (Nováková *et al.*, 2015). In the pyloric antrum, abundance of equidistantly spaced lymphoid follicles are found (Gelberg, 2001). Muscularis layer of the stomach comprises inner oblique, middle circular and outer longitudinal muscle layer, where myenteric plexus is found mostly in the middle circular muscularis layer. Lastly, mesothelium cells make up the serosa with an overlaid layer of loose connective tissue (Frappier, 2006).

## 2.3 Uses of Ultrasonography in Gastrointestinal Disorders

Ultrasonography is becoming a very common diagnostic imaging modality used in diagnosing gastrointestinal disorders in veterinary patients. Ultrasound is preferred over barium contrast after survey radiograph due its non-invasiveness in terms of ionizing radiation, real time imaging capabilities as well as zero risk of aspiration (Frame, 2006). Various changes to the echogenicity, wall layering and thickness of the gastrointestinal tract have been established to suggest signs of pathology (Roux *et al.*, 2016) Evaluation of the motility, luminal

content and wall symmetry are also important to be defined to characterize gastrointestinal disorders (Bru, 2002). Ultrasound, when utilized together with medical history, laboratory profile and other imaging modalities, can provide a more meaningful interpretation of the ultrasonographic images for accurate diagnosis of gastrointestinal diseases such as inflammatory bowel disease, lymphangiectasia, gastrointestinal lymphoma as well as intussusception (Nautrup *et al.*, 2000).

## 2.2 Ultrasonography of Gastric Layers

Ultrasonographically, the gastric layers which can be seen are conferred relatively to what can be seen in histology. The stomach is usually identified with the presence of rugal folds due to its position as the largest organ within the abdominal cavity (Penninck *et al.*, 2008). Landmark for the stomach in ultrasonography includes the liver at the left and mid abdomen. Positioning of the patients for gastric ultrasonography usually is at the dorsal recumbency with a supportive foam, but standing position have been documented to aid in displacing intraluminal gas dorsally when stomach is fluid filled (Nautrup *et al.*, 2000). Five layers of the stomach observed in ultrasonography begins with the lumen-mucosal interface which is hyperechoic. Subsequently the layers continue as hypoechoic mucosa, hyperechoic submucosa, hypoechoic muscularis and hyperechoic serosa. Thickness of the normal gastric layer in ultrasonography in cat have been documented with a reference range from 1.7mm to 3.6mm. However, measurements of the stomach layer pose as a challenge due to thickness differences between the rugal and interugal folds, which may also be affected by distension of the stomach (Penninck *et al.*, 2008). Stomach without ingesta may also portray rugal folds leading to false measurements of wall thickness, for which presentation of this in cats would be 'cauliflower'-like in ultrasonography (Nautrup *et al.*, 2000).

## 2.4 Pathologies associated to changes of gastrointestinal layers ultrasonographically

Changes in the layers of the mucosa and muscularis layer of the gastrointestinal tract ultrasonographically have been studied extensively. Examples of disease associated to changes in layer of mucosa with submucosal involvement include lymphocytic-plasmocytic enteritis, protein losing enteropathy and lymphangiectasia (Penninck, 2009). On the other hand, common diseases associated to changes in muscularis layer include inflammatory bowel disease (IBD) and gastric lymphoma (Daniaux *et al.*, 2014).

Lymphocytic-plasmocytic enteritis (LPE) is a commonly diagnosed gastrointestinal disorder in cats with reflection on modifications of the mucosal layer seen in ultrasonography. Thickening of the mucosal layer with comparison to other segments of intestine in the same animal, with increased uneven echogenicity and distortion of mucosa-submucosa demarcation have been described (Penninck, 2009). Apart from LPE, protein-losing enteropathy and lymphangiectasia have also been associated to changes in mucosal and submucosal layers on ultrasound. Dilated lacteals are commonly detected in these diseases, presented as mucosa layer with linear hyperechoic lines, perpendicularly to the luminal axis. Submucosa layer has been described to be thickened and uneven as well (Penninck, 2009).

Changes to the muscularis layer in ultrasound have been associated to diseases such as IBD and gastrointestinal lymphoma. These diseases have been reported to present similar ultrasonographic features of muscularis thickening of bowel wall, with retained wall layer architecture and no mass development. While other diseases may also be seen of have muscularis layer thickening, the ratio of the muscularis to submucosa layer have been suggested to be a useful marker for lymphoma and IBD infiltration in the gastrointestinal tract seen in ultrasonography (Daniaux *et al.*, 2014).

All the above studies have shown that changes in gastrointestinal layers in ultrasound do associate to gastrointestinal pathology, for which involvement of submucosa is usually present concurrent with other layers. However, isolated changes in gastric submucosa layer in ultrasound (GSM<sub>US</sub>) were never discussed.

## **2.5 Emerging Changes in Gastric Submucosal Thickness**

In recent years, there are increasing presentation of thickened GSM<sub>US</sub> of feline patients to the clinics. No literatures have documented the isolated changes in GSM<sub>US</sub>, hence the causes of these changes remain unknown. However, changes of GSM<sub>US</sub> concurrent with other layers such as mucosa have been associated to diseases like lymphangiectasia (Penninck, 2009). On the other hand, previous study on other imaging modalities have shown to be able to detect the deposition of fat in the gastric submucosa layer such as in radiograph and computed tomography (CT) scan (Heng *et al.*, 2005). With that, possibilities of involvement of pathology and fat deposition to the changes of GSM<sub>US</sub> may be present.

## **2.6 Gastric Submucosal Fat Detection by Radiograph and CT Scan**

Occasional intramural radiolucent band in the stomach wall detected on radiograph is associated to deposition of gastric submucosal fat (Ref). In radiograph, an intramural radiolucent band in the stomach wall is found in 33% of cats without any gastrointestinal diseases. Likewise in CT scan, an intramural hypoattenuating layer between the stomach serosal and mucosal surface which corresponds to Hounsfield unit of fat is found in 27% of cats without any gastrointestinal diseases. The intramural bands in the stomach seen on radiograph and CT are composed of fat deposited in the gastric submucosal layer using histology as a gold standard (Heng *et al.*, 2005), which is a normal finding in any healthy cats. Subsequently, another study has mapped out the distribution and prevalence of the gastric submucosal fat deposition using histology as a gold standard. The study concluded that 95%

of the cats sampled have deposited varying degrees of fat in the gastric submucosal layer (Heng *et al.*, 2008), which suggests that almost all cats, do deposit fat in the gastric submucosa. Studies on ability of ultrasound to detect gastric submucosal fat nor correlation studies of histology to ultrasound of the gastric submucosal layer have never been performed.

## **2.7 Gastric attachment to the adjacent organs**

Understanding the important attachments around the gastric pouch is crucial to a successful organ procurement. The gastric pouch is anatomically secured to its axis by various attachments including the greater and lesser omentum, as well as phrenoesophageal (or phrenicoesophageal) and gastrophrenic ligament (Dyce *et al.*, 2002). The phrenoesophageal ligament prevents the movement of the abdominal region of gastrointestinal tract from prolapsing into the thoracic cavity (Papazoglou *et al.*, 2014). The gastrophrenic ligament secures the fundus to the left crus of the diaphragm, while the greater omentum attaches the spleen against the greater curvature and the lesser omentum binds the lesser curvature to the liver (Dyce *et al.*, 2002).

### 3.0 MATERIALS AND METHODS

#### 3.1 Animals

25 cats euthanized for population control by the pound and shelter personnel were used in this study. Medical records were not available for all cats. Age was estimated by the pathologist (MM) based on dentition following guidelines by the Humane Society of United States (Fig. 1), where all cats were assumed to be adults. Carcasses obtained from the pound and shelter were immediately cooled in ice-packed ice box to be delivered to the examination facilities for further laboratory work.

<b><i>ESTIMATED AGE</i></b>	<b><i>CAT'S TEETH</i></b>
2-4 weeks	Deciduous (baby) incisors coming in
3-4 weeks	Deciduous (baby) canines coming in
4-6 weeks	Deciduous (baby) premolars coming in on lower jaw
8 weeks	All deciduous (baby) teeth are in
3½ - 4 months	Permanent incisors coming in
4-5 months	Permanent canines, premolars, and molars coming in
5-7 months	All permanent teeth in by 6 months
1 year	Teeth white and clean
1-2 years	Teeth may appear dull with some tartar build-up (yellowing) on back teeth
3-5 years	Teeth show more tartar build-up (on all teeth) and some tooth wear
5-10 years	Teeth show increased wear and disease; pigment visible on gums
10-15 years	Teeth are worn and show heavy tartar build-up; some teeth may be missing

Figure 1: Estimation Table of Dentition of Cats

### 3.2 Lipid Profiling

Blood samples were obtained after euthanasia through intracardiac puncture. Blood samples obtained were kept in plain blood tubes for at least 10 minutes before being centrifuged at 5000 rpm for 10 minutes to isolate the sera. Sera was separated and stored frozen in -80°C until future usage to measure triglyceride and cholesterol concentrations at the in-house Clinical Pathology Laboratory.

### 3.3 In-vivo Ultrasound

A single operator (LSY) performed the in-vivo B-mode ultrasound (US) examinations. The linear transducer (My Lab Class C, LA533 electronic linear transducer 3-13MHz, Esaote, Florence, Italy) used for the B-mode US was lined with acoustic coupling gel followed by single layered cling wrap to protect the probe. The carcasses were placed in dorsal recumbency on a covered padded trough and the fur of the ventral abdomen from xiphoid, along the costal arch on both sides towards the pubis was clipped. Water was sprayed over the ventral abdomen to reduce gas interphase and acoustic coupling gel was applied to the skin prior abdominal ultrasound. Images of the stomach were obtained ultrasonographically to determine distension degree of each sample prior to stomach procurement. Images were acquired using the linear transducer. Orientation of the image was consistent for all samples scanned. The abdomen was scanned at the longitudinal section along the ventral surface of abdomen using the transducer from the fundus to the pylorus. Following that, the abdomen was scanned at the transverse section along the ventral abdomen from the fundus to the pylorus (Barr *et al.*, 2011).

### **3.4 Organ Procurement**

For each cat, the oesophagus was resected as orad as possible by dissecting through the thoracic cavity of the cat using Metzenbaum scissors to expose the diaphragm and the esophagus in the thoracic cavity. The phrenoesophageal ligament was severed to isolate the esophagus from the esophageal hiatus. The esophagus was then auto-ligated as orad as possible. The stomach was isolated by severing multiple ligaments including the gastrophrenic ligament, the lesser omentum and greater omentum which joins the fundus to the left crus of diaphragm, less curvature to liver and greater curvature to the spleen (Dyce, 2003) The esophagus was ligated with 1/0 silk using surgeon's knot suture pattern as orad as possible to prevent leakage of the ingesta. The aborad region of the stomach was isolated at about 3cm from the pyloric antrum at the proximal portion of the descending duodenum. Thereafter, the proximal duodenum was ligated with 1/0 silk using surgeon's knot suture pattern. About 1cm thickness of mesentery was preserved around the stomach at the greater curvature, lesser curvature and pylorus to allow anchoring of the stomach to the paraffin tray using 25-G needles.

### **3.5 Ex-vivo Ultrasound**

A single operator (LSY) who performed the in-vivo B-mode US also performed the ex-vivo US examinations. The paraffin tray containing the stomach was filled with water until about 1 to 2 cm above the surface of the isolated stomach to serve as an anechoic coupling medium to the stomach sample and prevent ultrasonographic beam reflection caused by air. The stomach was imaged at the fundus, body, and pylorus (Fig. 2) within the water bath, about 1 cm from the serosal surface of the stomach, parallel to the paraffin tray without direct contact of the ultrasound probe to the ventral stomach surface in order to avoid pressure application on the stomach. The ultrasound focus was set at the level of the stomach wall. Digital calliper of the US machine was used to mark the site of gastric wall which had the clearest stomach layers

(mucosa, submucosa, muscularis and serosa). Guided by ultrasound, two 22-G needles were placed at approximately 45-degree angle on each side of the greater and lesser curvature of the stomach sample, without penetration of the stomach wall. This was done to mark the site where the transverse ultrasonographic images were obtained, for which histological transverse sections were also taken at the same level for higher relevance of comparison. Still ultrasonographic images of the sample were taken with the presence of needle to indicate the specific site of interest to be acquired for measurement.

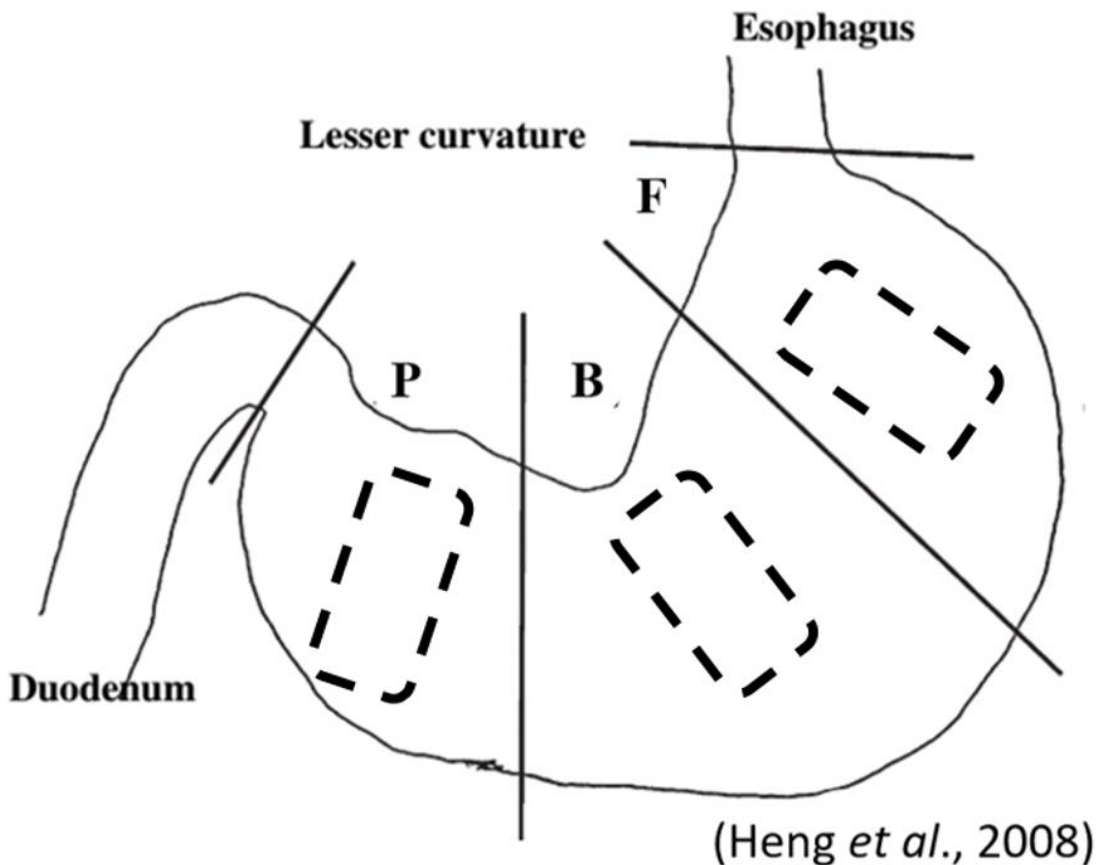


Figure 2: Three different regions of ultrasonographic imaging. F = fundus, B = body, P = Pylorus. Dotted lines referred to the ventral sites of the stomach where histological samples were retrieved.

### 3.6 Histology

Immediately following ultrasonographic images acquisition, the stomach was then resected to retrieve the histological samples. The ventral surface of the stomach (Fig.2) was resected from each regions (fundus, body, and pylorus) according to the marked sites of the 22-G needles. Each sample was approximately 5 to 6 cm in length and 2 to 3 cm in width. Each strip was laid on paper towel with the mucosa surface facing up and labelled with the region obtained on the paper towel using ball pen. The sample was then submerged in a 10% neutral buffered formalin filled sampling container. Post formalin tissue fixation for more than 48 hours, the sample was processed routinely, embedded in paraffin, sectioned with the microtome at 4  $\mu\text{m}$  thickness, stained with hematoxylin and eosin and lastly mounted with DPX (distyrene, plasticiser and xylene). The histological sections were then assessed and photomicrographs were taken using a research grade light microscope equipped with image analyser (Nikon Image Analysis System NIS-Elements Documentation Version 33.2, Selangor, Malaysia) for histological evaluation later.

### 3.7 Quantitative Analysis

The ultrasonographic images exported and saved as bitmap images were analysed by a single operator (TYB) using an image analysis system (Image J). Photomicrographs taken from the histological slides were exported as tag image file format (TIFF) to be analysed using the same image analysis system (Image J). This system measures the number of pixels within a given distance or boundary. With respect to the scale bar provided by each imaging system on the images exported either from ultrasound in centimetres (cm) or digital histology scanner in micrometres ( $\mu\text{m}$ ), the pixels were easily converted into desired units for accurate comparison.

In each ultrasound image, the total thickness of the stomach layer was measured at the area with best visualization of all five gastric layers with respect to the digital caliper placed

by the B-mode US machine operator (LSY). Then, the thickness of the hyperechoic submucosa layer was measured at five different regions randomly where the layers of the stomach were best visualized in order to obtain the average thickness of the submucosal layer by the image analysis operator (TYB). Presence of rugae folds in each ultrasound image was also evaluated.

In each histological slide, five views of the slide were captured and analysed at the magnification of the objective lens at 4x. For each view, the total thickness of the stomach histology layer was measured at the point of the deepest gastric pit to the serosa if seen on histology, or the tunica muscularis if serosa was not seen on histology. The thickness of the submucosa layer was measured at five different regions of the view randomly to obtain an average thickness. Total area of the submucosa and the area of fat globules within the submucosa in each view was also taken. This was to allow the tabulation of fat percentage within the submucosa layer using the formula:

$$\text{Fat Percentage in Submucosal Layer} = \frac{\text{Area of Fat in Submucosa Layer}}{\text{Area of Submucosa Layer}}$$

The average thickness of the total stomach layer and submucosal layer, average area of submucosa and its fat globules as well as fat percentage were then calculated from the five different views of the same histology slide. The continuous data of fat percentage was then assigned a fat score (Fig. 3).

Score	Criteria
0	No fat
1	<1% fat in submucosa layer area
2	Fat from 1 - 25% in submucosa layer area
3	Fat from 25% - 50% in submucosa layer area
4	Fat from 50% - 75% in submucosa layer area
5	Fat from 75% - 100% in submucosa layer area

Figure 3: Fat score table derived from Heng *et al.*, 2008.

### 3.8 Statistical Analysis

Statistical analysis program, IBM SPSSv.22 was used for statistical analysis. Normality of the data was assessed using Shapiro-Wilk test. Correlation test of the gastric submucosal thickness in histology was compared against the gastric submucosal thickness in ultrasound using Pearson's Correlation Coefficient. Ultrasound thickness of the gastric submucosa was compared against the fat score derived from area of submucosal fat in histology using ANOVA. The triglyceride and cholesterol level were compared against the fat score derived from area of submucosal fat in histology using ANOVA. Paired T-test was used to compare the gastric submucosal thickness to the presence of rugae fold. A P-value of  $< 0.05$  was considered as statistically significant.

## **4.0 RESULTS**

### **4.1 Animals**

All of the cats included in the study were Domestic Short Hair (DSH) breed. Sex distribution of the cats were 10 intact females and 15 intact males. A total of 16 cats were received from the federal cat pound while 9 cats were received from a collaborating animal shelter.

### **4.2 Stomach samples**

Twenty-five stomach samples were available for ultrasound scanning and interpretation at the regions of fundus, body and pylorus. Through ultrasound-guidance, 75 stomach samples were available for histological processing and interpretation.

### **4.3 Histology samples**

Three histological samples were obtained from each stomach sample comprising the fundus, body and pylorus, resulting in a total of 75 histological slides for analysis.

### **4.4 Statistical Analysis**

Mean thickness and range values for the total gastric layer thickness and gastric submucosal thickness on each region of the stomach on ultrasound and histology are shown in Table 1. Distribution of the fat in gastric submucosa layer according to the fat score are shown in Table. 2. The correlation between the gastric submucosal layer thickness between ultrasonography and histology using a two-tailed Pearson's Correlation test (Table 3) showed a significant moderate relationship in the body ( $r = 0.459$ ,  $P = 0.021$ ) but not in the fundus and pylorus ( $P > 0.05$ ). Associated scatterplots for each region of the gastric submucosal layer measurements on ultrasonography against histology are shown in Figs. 1, 2 and 3. There was a statistically significant difference between the gastric submucosal layer thicknesses in

ultrasonography at the presence or absence of gastric rugae fold in the fundus and body region, but not the pylorus region as shown in Table 4. There was no statistically significant association between the gastric submucosal layer measurements in ultrasonography and gastric submucosal fat score measurements in histology in all regions as shown in Table 5.-There was also no statistically significant association between serum lipid parameters and gastric submucosal fat score measured in histology as shown in Table 6.

Table 1. Thickness of the Fundus, Body and Pylorus Wall Layers Measured in Ultrasonography and Histologically

	Fundus (n = 25)		Body (n = 25)		Pylorus (n = 25)	
	Mean $\pm$ SD (mm)		Mean $\pm$ SD (mm)		Mean $\pm$ SD (mm)	
	[Range (mm)]		[Range (mm)]		[Range (mm)]	
	Ultrasound	Histology	Ultrasound	Histology	Ultrasound	Histology
Submucosa	0.690 $\pm$ 0.298 [0.204-1.494]	0.400 $\pm$ 0.180 [0.213-0.857]	0.694 $\pm$ 0.284 [0.246-1.650]	0.347 $\pm$ 0.147 [0.163-0.844]	0.574 $\pm$ 0.127 [0.296-0.902]	0.206 $\pm$ 0.091 [0.083-0.547]
Total Thickness	2.457 $\pm$ 0.857 [0.930-4.960]	1.618 $\pm$ 0.445 [0.879-2.546]	2.678 $\pm$ 1.046 [1.220-5.530]	1.675 $\pm$ 0.321 [1.146-2.370]	2.127 $\pm$ 0.609 [0.259-3.320]	1.609 $\pm$ 0.287 [0.931-2.114]

Table 2: Distribution of Fat Score in Submucosa Layer in different regions of the stomach

Region	Score 0	Score 1	Score 2	Score 3	Score 4	Score 5	n
Fundus	1 (4%)	1 (4%)	11 (44%)	6 (24%)	6 (24%)	0	25 (100%)
Body	1 (4%)	2 (8%)	5 (20%)	8 (32%)	9 (36%)	0	25 (100%)
Pylorus	5 (20%)	4 (16%)	10 (40%)	5 (20%)	1 (4%)	0	25 (100%)

Table 3: Correlation of Gastric Submucosa Layer Thickness between Ultrasonography and Histology

	Fundus (n = 25)	Body (n = 25)	Pylorus (n = 25)
Pearson correlation, $r^\dagger$	0.191	0.459	0.293
Significance (two-tailed)	$P = 0.360$	$P = 0.021^*$	$P = 0.155$

\*Correlation is significant at the 0.05 level (two-tailed)

$^\dagger$ According to British Medical Journal, with absolute values of  $r$ , 0-0.19 is regarded as very weak, 0.2-0.39 as weak, 0.40-0.59 as moderate, 0.6-0.79 as strong and 0.8-1 as very strong correlation

Table 4: Gastric Submucosal Thickness on Ultrasonography (GSM<sub>US</sub>) and Presence of Rugae Fold

Rugae Fold	GSM <sub>US</sub> Thickness		P-value
	Present	Absent	
Fundus (n=25)	0.879 ± 0.313 [0.434 - 1.494]	0.563 ± 0.215 [0.204 - 0.892]	0.006**
Body (n=25)	0.831 ± 0.345 [0.436 - 1.650]	0.587 ± 0.170 [0.246 - 0.860]	0.030*
Pylorus (n=25)	0.614 ± 0.135 [0.460 - 0.902]	0.548 ± 0.118 [0.296 - 0.716]	0.205

\*Significant at the 0.05 level (two-tailed)

\*\* Significant at the 0.01 level (two-tailed)

Table 5: Association between Gastric Submucosal Layer Thickness in Ultrasonography (GSM<sub>US</sub>) to Gastric Submucosal Fat Score in Histology

GSM <sub>US</sub> Thickness [Mean ± SD/Range(mm)]	Gastric Submucosal Fat Score					P-value
	0	1	2	3	4	
Fundus (n=22)	N/A	N/A	0.618 ± 0.279 [0.204 - 1.184]	0.894 ± 0.404 [0.434 - 1.494]	0.621 ± 0.178 [0.324 - 0.770]	0.175
Body (n=22)	N/A	N/A	0.653 ± 0.122 [0.484 - 0.776]	0.633 ± 0.203 [0.386 - 0.894]	0.812 ± 0.396 [0.392 - 1.650]	0.398
Pylorus (n=24)	0.485 ± 0.098 [0.346 - 0.618]	0.539 ± 0.014 [0.524 - 0.555]	0.619 ± 0.167 [0.296 - 0.902]	0.599 ± 0.084 [0.512 - 0.696]	N/A	0.270

Table 6: Association between Serum Lipid Parameters to Gastric Submucosal Fat Score Measurements in Histology

Lipid Parameters [Mean ± SD/Range(mmol/L)]	Reference Range (mmol/L)	Gastric Submucosal Fat Score					P-value
		0	1	2	3	4	
Cholesterol (n=22)	3.7-17.6	N/A	2.2 ± 0.6 [1.2 - 3.2]	3.6 ± 1.9 [2.4-6.8]	2.5 ± 2.0 [0.8-6.3]	N/A	0.192
Triglyceride (n=22)	1.4-7.4	N/A	0.8 ± 0.2 [0.5 - 1.2]	1.5 ± 0.8 [0.8 - 2.7]	1.3 ± 1.5 [0.3 - 4.4]	N/A	0.233

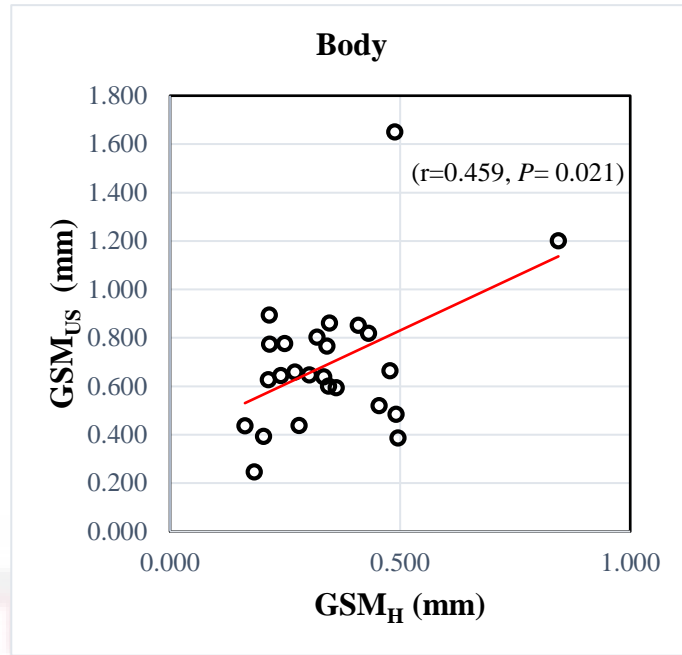


Figure 1: Scatterplot of GSM<sub>US</sub> against GSM<sub>HS</sub> in the body region.

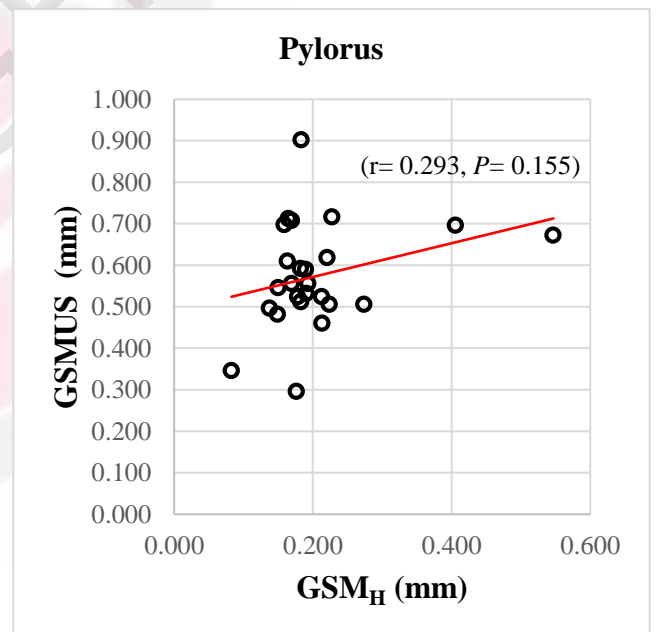
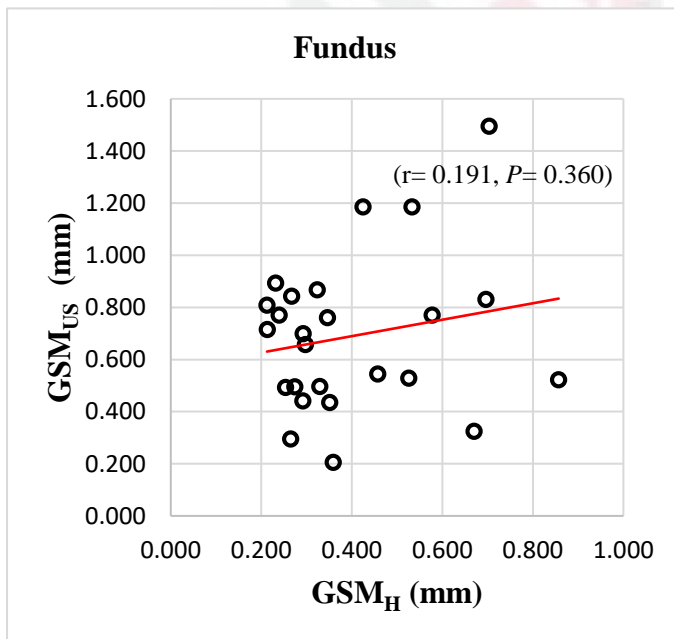


Figure 2 and 3 : Scatterplots of GSM<sub>US</sub> against GSM<sub>HS</sub> in the fundus and pylorus region.

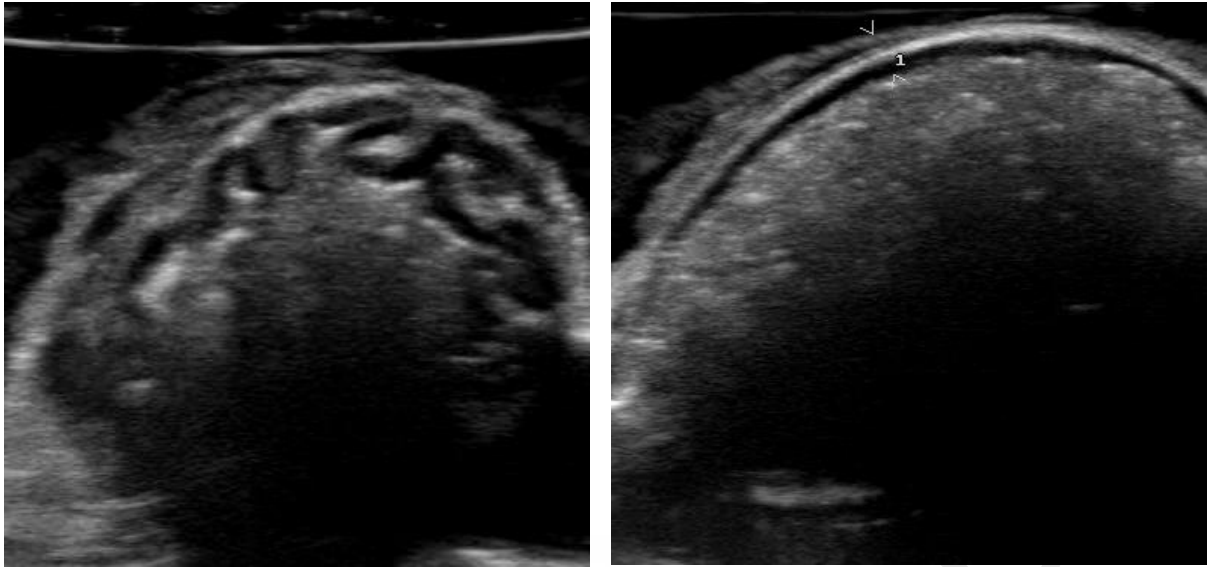


Figure 4 and 5: Ultrasonographic images of gastric with presence (left) and absence (right) of rugae folds.

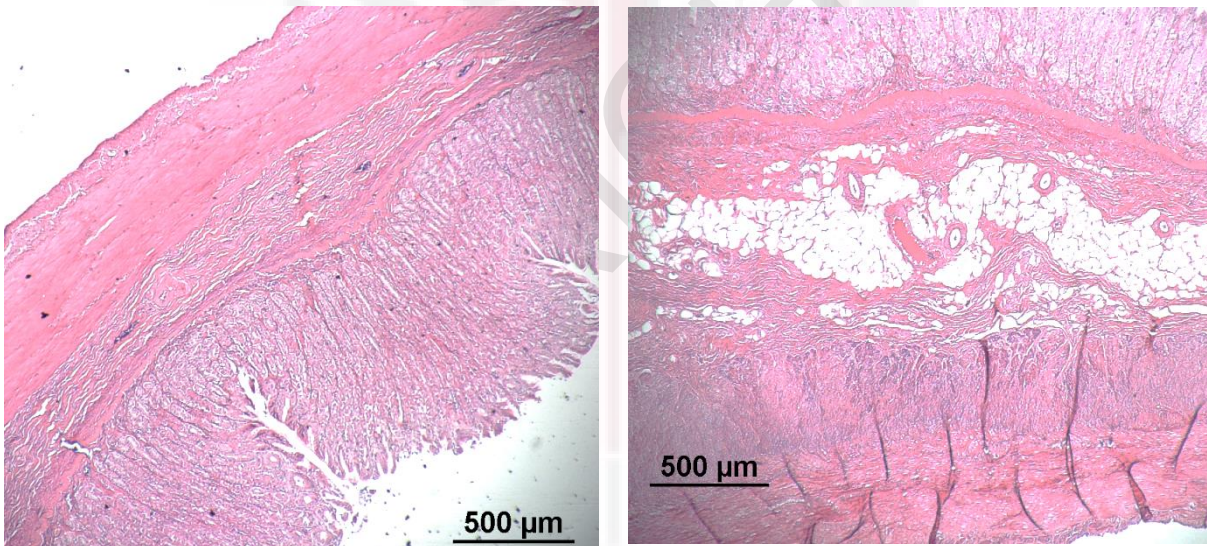


Figure 6 and 7: Histological images of gastric submucosa with fat score of 0 (left) and 4 (right).

## 5.0 DISCUSSION

In our study, 96% of the cats sampled deposited varying degree of fat in the gastric submucosa. The body of the stomach had the highest tendency to deposit fat, while the pylorus had the least. Moderate correlation between the gastric submucosal layer thickness measured on ultrasonography and histology was present ( $r = 0.459$ ,  $P = 0.021$ ) in the body. Significant difference was found between gastric submucosal layer thicknesses measured on ultrasound when rugae fold was present or absent. However, no significant association was found between the gastric submucosal layer thickness measured on ultrasonography and gastric submucosal fat score measured in histology. Additionally, no significant association was found between serum lipid parameters and the gastric submucosal fat measured in histology.

This study revealed that 24 out of 25 cats (96%) deposited varying degrees of fat in the gastric submucosal layer of different stomach regions. This finding was similar to the findings by Heng *et al.*, 2008 where 95% of their samples deposited varying degrees of fat in the gastric submucosal layer. Among the three regions of the stomach, the body had the highest tendency to deposit fat, as 36% of the samples scored a fat score of 4, the highest percentile between the three regions and within the body region. In contrast, pylorus had shown to have the least tendency to deposit fat, as 20% of the samples scored a fat score of 0, the highest percentile between the three regions of the stomach. The stark contrast of the fat deposition may be due to the anatomical correlation of the function of the regions. The body serves as a mixing region of the stomach for optimal ingesta and gastric juice digestive processes (Dyce *et al.*, 2002), the fat deposition may have served as a mechanical buffer, as to fat deposited in a fibrous lattice in the dog's footpad (Dyce *et al.*, 2002). However, the clear function of the submucosal fat is yet to be determined (Heng *et al.*, 2008). The pylorus is the junction between the stomach and duodenum which helps propel the ingesta at a controlled rate, with increased muscular fold towards the pyloric sphincter (Dyce *et al.*, 2002). Folding of the muscularis layer into the

submucosa and mucosa layer to form the pyloric sphincter may have resulted in a lesser tendency to deposit fat in this region.

Correlation between the gastric submucosal layer thickness between ultrasonography and histology was significant in our studies, showing that changes in the thickness on histology was well reflected on ultrasonography. This significant correlation was shown to be moderate only in the region of the body but not the fundus nor pylorus. This could be due to the ease of scanning the body of the stomach, leading to accurate measurement of its thickness when compared to the fundus or pylorus. Discrepancies of the measurements in the fundus and pylorus region ultrasonographically may be contributed by the low margin of error as both regions make up a lower area of the stomach.

From our study, the thickness of the gastric submucosal layer was significantly different with the presence or absence of rugae fold. This was evident in the fundus and body region, but not the pylorus. As the degree of gastric distension will affect the visibility and thickness of the gastric rugae of the fundus and body (Armburst, 2011), this would also be reflected in the ultrasonographic findings of the gastric submucosal layer measurement as well. However, this was not found in the pylorus due to its low distension degree as compared to the other regions (Dyce *et al.*, 2002), hence changes of the ultrasound measurement of the gastric submucosal layer was not affected by the presence of rugae folds.

Significant association between the gastric submucosal layer thickness in ultrasonography and the fat score on histology was not present in our studies. While fat deposition in the gastric submucosa have been shown to be the primary reason for the presence of intramural bands seen on radiograph and CT scans (Heng *et al.*, 2005), our study have shown that the varying degree of fat deposition did not cause significant changes to the gastric submucosal layer thickness in cats. This may be contributed by varying degree of gastric

distension overshadowing the effects of gastric submucosal fat deposition on the changes of the gastric submucosal layer thickness on ultrasound.

Finally, serum lipid parameters in each cat have showed no significant association to the gastric submucosal fat measurements in histology. This meant that the lipid profile of the cat did not influence the amount of fat deposited in the gastric submucosa. As both cholesterol and triglyceride only provide the indication of lipid levels which are being transported at a single point in time, they do not provide the degree of fat deposition in the body (Cornell University College of Veterinary Medicine, 2013). A more reliable test for fat deposition in the body is the test for diacylglycerol acyltransferase (DGAT) enzyme, which functions to esterify triglyceride in the body to lipid droplets to be stored as fat (Yen *et al.*, 2008). As we were not able to obtain the body condition score and body weight of the samples, cholesterol and triglyceride were the most common parameters available from the serum to detect the lipid profile of the animals.

## 6.0 CONCLUSION

The findings in our study have concluded that there was a correlation between the gastric submucosal thickness measurements in ultrasonography and histology, which was moderately significant in the body of the stomach. Apart from that, presence of rugae folds was associated to the changes of the gastric submucosal measurements in ultrasound. This means that gastric distension, presented as absence of rugae folds in ultrasonography have caused the significant changes in the thickness of gastric submucosa in ultrasonography. Association was not found between the gastric submucosal measurements in ultrasonography and the gastric submucosa fat score measurements in histology. Hence, fat deposition was not the cause of the changes in thickness of gastric submucosa seen in ultrasonography.

## REFERENCES

Ahualli, J. (2007). The Fat Halo Sign 1. *Radiology*, 242(3), 945-946.

Akers, R. M., & Denbow, D. M. (2008). *Anatomy and physiology of domestic animals* (2nd ed.). Ames, Iowa: Blackwell.

Anderson, K. (2011). Ultrasonography of the GI Tract. Retrieved November 14, 2016, from <http://www.academic-server.cvm.umn.edu/radiology/CVM6105/2011/Anderson/pdf/USofGI.pdf>

Armburst, L. J. (2011, August 01). Ultrasonography of the gastrointestinal tract: a myriad of disease (Proceedings). Retrieved March 3, 2017, from <http://veterinarycalendar.dvm360.com/ultrasonography-gastrointestinal-tract-myriad-disease-proceedings>

Barr, F., & Gaschen, L. (2011). *BSAVA manual of canine and feline ultrasonography*. Quedgeley, Gloucester: British Small Animal Veterinary Association.

Cohen, M., Post, G. S., & Wright, J. C. (2003). Gastrointestinal leiomyosarcoma in 14 dogs. *Journal of veterinary internal medicine*, 17(1), 107-110.

Couto, C. G., Rutgers, H. C., Sherding, R. G., & Rojko, J. (1989). Gastrointestinal lymphoma in 20 dogs. *Journal of Veterinary Internal Medicine*, 3(2), 73-78.

Cornell University College of Veterinary Medicine. (2013). Lipid Overview. Retrieved March 5, 2017, from <http://www.eclinpath.com/chemistry/energy-metabolism/lipid-overview/>

Daniaux, L. A., Laurenson, M. P., Marks, S. L., Moore, P. F., Taylor, S. L., Chen, R. X., & Zwingenberger, A. L. (2014). Ultrasonographic thickening of the muscularis propria in feline small intestinal small cell T-cell lymphoma and inflammatory bowel disease. *Journal of feline medicine and surgery*, 16(2), 89-98.

Frame, M. (2006). Gastro-intestinal tract including pancreas. *Diagnostic Ultrasound in Small Animal Practice*, 90-92.

Frappier, B. L. (2006). *Dellmann's Textbook of Veterinary Histology* (6th ed.). Ames, Iowa: Blackwell.

Gervaise, A., Naulet, P., Gervaise-Henry, C., Junca-Laplace, C., Pernin, M., & Lapierre-Combes, M. (2016). Gastric Wall Fatty Infiltration in Patients Without Overt Gastrointestinal Disease. *American Journal of Roentgenology*, 206(4), 734-739.

Gillespie, V., Baer, K., Farrelly, J., Craft, D., & Luong, R. (2011). Canine gastrointestinal stromal tumors: immunohistochemical expression of CD34 and examination of prognostic indicators including proliferation markers Ki67 and AgNOR. *Veterinary pathology*, 48(1), 283-291.

Hee-Chun, L. E. E., Ji-Hyun, K. I. M., Cho-Hee, J. E. E., Jae-Hoon, L. E. E., Jong-Hyun, M. O. O. N., Na-Hyun, K. I. M., ... & Dong-In, J. U. N. G. (2014). A case of gastric adenocarcinoma in a Shih Tzu dog: successful treatment of early gastric cancer. *Journal of Veterinary Medical Science*, 76(7), 1033-1038.

Heng, H. G., Wrigley, R. H., Kraft, S. L., & Powers, B. E. (2005). Fat is responsible for an intramural radiolucent band in the feline stomach wall. *Veterinary Radiology & Ultrasound*, 46(1), 54-56.

Jubb, K. V., Kennedy, P. C., & Palmer, N. (1985). *Pathology of Domestic Animals* (3rd ed., Vol. 2). Orlando, Florida: Academic Press.

Katsianou, I., Svoronou, M., & Papazoglou, L. G. (2014, August). Current views regarding hiatal hernia in dogs and cats. Retrieved Feb. & march, 2017, from [http://hcam.hcavs.gr/images/vol3iss2/izs\\_vol3\\_issue2\\_hiatal-hernia.pdf](http://hcam.hcavs.gr/images/vol3iss2/izs_vol3_issue2_hiatal-hernia.pdf)

King, D. (2009, October 7). Histology of the Gastrointestinal System. Retrieved March 3, 2017, from <http://www.siumed.edu/~dking2/erg/giguide.htm#meissner>

Larson, M. M., & Biller, D. S. (2009). Ultrasound of the gastrointestinal tract. *Veterinary Clinics of North America: Small Animal Practice*, 39(4), 747-759.

Nautrup, C. P., & Tobias, R. (2000). *An Atlas and Textbook of Diagnostic Ultrasonography of the Dog and Cat* (1st ed.). London: CRC Press.

Nováková, L., & Blanková, B. (2015). Functional Morphology of the Gastrointestinal Tract. Retrieved March 3, 2017, from <http://fblt.cz/en/skripta/ix-travici-soustava/1-funkcni-morfologie-travici-trubice/>

Parrah, J. D., Moulvi, B. A., Gazi, M. A., Makhdoomi, D. M., Athar, H., Dar, S., & Mir, A. Q. (2013). Gastric ulceration in dog: A review. *World*, 6(7), 449-454.

Penninck, D. G., Moore, A. S., & Gliatto, J. (1998). Ultrasonography of canine gastric epithelial neoplasia. *Veterinary Radiology & Ultrasound*, 39(4), 342-348.

Penninck, D., & D'anjou, M. (2008). *Atlas of Small Animal Ultrasonography* (2nd ed.). Ames, Iowa: Blackwell.

Peters, R. M., Goldstein, R. E., Erb, H. N., & Njaa, B. L. (2005). Histopathologic features of canine uremic gastropathy: a retrospective study. *Journal of veterinary internal medicine*, 19(3), 315-320.

Thomson, R. G., McGavin, D. M., Carlton, W., & Zachary, J. F. (2001). *Thomson's Special Veterinary Pathology* (3rd ed.). Mosby.

Yam, P. S., Johnson, V. S., Martineau, H. M., Dickie, A., & Sullivan, M. (2002). Multicentric lymphoma with intestinal involvement in a dog. *Veterinary Radiology & Ultrasound*, 43(2), 138-143.

Yen, Chi-Liang Eric, et al. "Thematic review series: glycerolipids. DGAT enzymes and triacylglycerol biosynthesis." *Journal of lipid research* 49.11 (2008): 2283-2301.

